Magnetism and the absence of superconductivity in the praseodymium–silicon system doped with carbon and boron

J. de la Venta [a,*], Ali C. Basaran [a,b], T. Grant [c], J.M. Gallardo-Amores [d], J.G. Ramirez [a], M.A. Alario-Franco [d], Z. Fisk [c], Ivan K. Schuller [a]

[a] Department of Physics and Center for Advanced Nanoscience, University of California, La Jolla, San Diego, CA 92093, USA
[b] Materials Science and Engineering, University of California, La Jolla, San Diego, CA 92093, USA
[c] Department of Physics and Astronomy, University of California, Irvine, CA 92697, USA
[d] Departamento de Quimica Inorganica I, Universidad Complutense, E-28040 Madrid, Spain

ABSTRACT

We searched for new structural, magnetic and superconductivity phases in the Pr–Si system using high-pressure high-temperature and arc melting syntheses. Both high and low Si concentration areas of the phase diagram were explored. Although a similar approach in the La–Si system produced new stable superconducting phases, in the Pr–Si system we did not find any new superconductors. At low Si concentrations, the arc-melted samples were doped with C or B. It was found that addition of C gave rise to multiple previously unknown ferromagnetic phases. Furthermore, X-ray refinement of the undoped samples confirmed the existence of the so far elusive Pr_3Si_2 phase.

© 2013 Elsevier B.V. All rights reserved.

1. Introduction

We investigated the Pr–Si system using high-pressure high-temperature (HP–HT) and arc melting syntheses with C and B doping. Following our previous search for superconductors in the La–Si system [1], we have extended the study to Pr–Si compounds. While much work has been done on the phase diagram of binary Pr-silicides, there are still a number of open questions [2]. For example, before this work, the existence of Pr_3Si_2 was uncertain. The presence of Pr_3Si_2 was first reported in Ref. [3], but has not been reproduced in more recent studies [2,4,5]. Magnetic and electrical properties of the binary system have also been extensively studied [5]. In the binary system there are six ferromagnetic compounds showing different Curie temperatures (T_C): Pr_5Si_3 ($T_C = 42$–44 K) [5–7], Pr_5Si_4 ($T_C = 40$ K) [5], PrSi ($T_C = 51$–54 K) [5,8], Pr_3Si_4 ($T_C = 100$–105 K) [5,9], Pr_3Si_5 ($T_C = 11.5$ K) [10] and $PrSi_2$ ($T_C = 11.5$ K) [11], as well as one antiferromagnetic compound, $PrSi_{2-x}$ ($x = 0.12$), with the Neel temperature $T_N = 11$ K [5].

Our study includes two different regions of the phase diagram. To investigate the high Si concentration compounds, the $PrSi_2$ phase with an excess of Si was synthesized by HP–HT. High pressure synthesis is a unique technique which allows

incorporation of elements into compounds which otherwise cannot be synthesized at ambient pressure. This technique, together with electron and hole doping, is commonly used to produce new superconductors [12,13]. It has been recently found that by HP–HT synthesis it is possible to stabilize two new superconducting compounds in the La–Si system: $LaSi_5$ and $LaSi_{10}$ with critical temperatures of 11.5 and 6.7 K respectively [14]. To explore the high Pr concentration binary compound Pr_5Si_3, we have synthesized by arc-melting Pr_5Si_3 undoped and doped with C or B.

2. Experimental

2.1. Synthesis

For HP-HT synthesis of the Si highest concentration compounds, first $PrSi_2$ samples were prepared by arc-melting. Then, the $PrSi_2$ samples were grounded and mixed with Si (99.9995%) powders to obtain the nominal composition $PrSi_5$. Finally the powders were synthesized by placing them in a Pt capsule in air atmosphere and compressed to 80 Kbar at 1100 °C for 30 min in a Belt type press.

To study the high Pr concentration phases, multiphase samples were prepared by arc-melting the constituents on a water-cooled copper hearth under purified argon atmosphere. High purity Pr

(99.95%), Si (99.9995%), B and graphite chips (99.9995%) were used. Eight different polycrystalline samples with the following nominal compositions were prepared: Pr_5Si_3 (undoped sample), $Pr_5Si_3B_{0.3}$, Pr_5Si_3B, $Pr_5Si_3C_{0.3}$, Pr_5Si_3C, $Pr_5Si_3C_{1.5}$, $Pr_5Si_3C_2$ and $Pr_5Si_3C_3$. The samples were turned and remelted four times to ensure homogeneity. Total weight loss after arc-melting was less than 0.4%. After melting, the samples were wrapped in tantalum foil and sealed in evacuated quartz tubes for further annealing at 1000 °C for 5 days.

2.2. X-ray powder diffraction (XRD)

The synthesized metallic pellets were grounded into a fine powder using an agate mortar and pestle to avoid preferred orientation which may produce misleading diffraction patterns. In-house XRD was initially Cu-Kα radiation. High resolution synchrotron powder diffraction (HRXRD) data were measured in a transmission capillary geometry using the mail-in program at beamline 11-BM of the Advanced Photon Source (APS), at Argonne National Laboratory, with a wavelength of 0.41352 Å. Discrete detectors covering an angular range from $2\theta = -6°$ to $16°$ were scanned over a $34°$ 2θ range, with data points collected every $0.001°$ at a rate of 0.01 deg/s [15–17]. For the Rietveld refinement we used the EXPGUI software [18], a graphical interface for the GSAS package [19].

2.3. Magnetic characterization

Magnetic properties were characterized using a Quantum Design MPMMS SQUID magnetometer. For Zero Field Cooled-Field Cooled (ZFC-FC) magnetizations, the applied magnetic field was 100 Oe and the temperature was scanned in the 5–100 K range. In addition, dependence of magnetization on applied field was measured at different temperatures.

2.4. Magnetic field modulated microwave spectroscopy (MFMMS)

MFMMS is a unique technique that allows detection of minuscule superconducting regions in inhomogenous systems faster and with higher sensitivity than most conventional methods [1,20]. MFMMS is based on a measurement of temperature dependent phase sensitive microwave absorption while the sample is subjected to an AC modulated magnetic field. The AC field modulation together with phase sensitive detection is known to produce a sharp peak-like behavior across the superconducting transition [1,20]. The superconducting onset temperature is correlated with the temperature at which the MFMMS signal falls below the background noise level. Non-superconducting transitions (pure magnetic transitions) have a different response at microwave frequencies. The absorption is dominated by the change of the surface resistance and skin depth as opposite on the SC transitions where the main absorption mechanism arises from the expulsion of the magnetic flux on the Meissner state [21].

3. Results and discussion

3.1. High pressure–high temperature synthesized Pr_5Si_2

XRD measurements show that the starting material (arc-melted $PrSi_2$) is single phase tetragonal $PrSi_2$ with space group I41/amd (Fig. 1). Magnetic properties of this phase (Fig. 2a) are consistent with previously reported data and show a FM transition at 11 K [11]. The FC curve of the magnetization data shows a drop. The Curie temperature T_C is estimated from the midpoint of this drop. The peak observed in the ZFC curve is related to the Hopkinson effect (or Hopkinson peak) [22,23]: due to a decrease
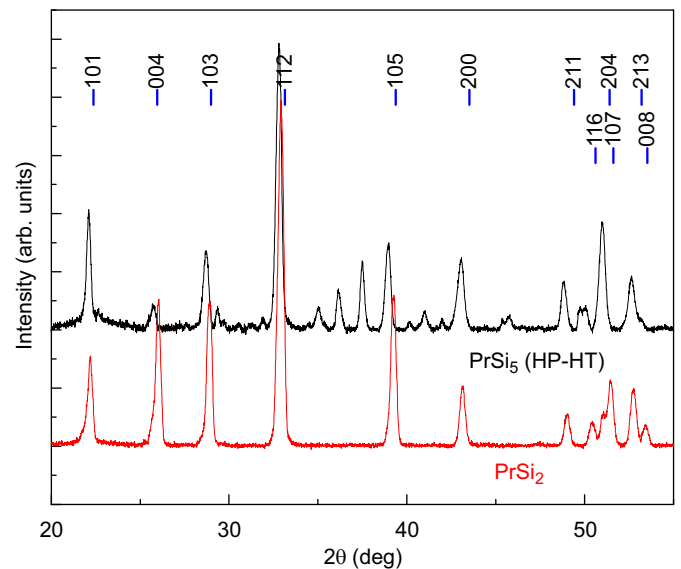
Fig. 1. X-ray diffraction patterns for: (bottom red) starting material $PrSi_2$; (top black). Intended composition $PrSi_5$ after HP–HT synthesis. Tick marks indicate reflections coming from the $PrSi_2$ phase. (For interpretation of the references to color in this figure legend, the reader is referred to the web version of this article.)

in the anisotropy before the magnetic order disappear the initial magnetization increases with increased temperature and exhibits a sharp maximum just below the Curie temperature.

After the HP–HT synthesis new XRD peaks appear (Fig. 1), and the maxima coming from the $PrSi_2$ phase remains. All of the new XRD peaks could be attributed to intermetallic Pt-Si phases: $Pt_{12}Si_5$, $PtSi$ and Pt_6Si_5. This indicates that the Pt capsule used in the HP–HT synthesis is reacting with the materials. In contrast to the La–Si system [14], no sign of the formation of a new $PrSi_5$ phase has been found. After the HP–HT synthesis the $PrSi_2$ XRD peaks are shifted, Fig. 1. The shift towards lower values is more pronounced in the planes along the z direction (notice, for example, the small shift in the (200) plane compared to the larger shift in the (004) plane). This shift indicates a change in the lattice parameter c, from 13.65 Å in the starting material to 13.84 Å in the HP–HT sample.

Magnetic characterization of the HP–HT sample (Fig. 2b), shows a strong paramagnetic component. The splitting of ZFC and FC magnetization curves at ~11 K indicates that the original FM component is still present. After the HP–HT synthesis the magnetization values at 5 K are reduced by an order of magnitude. This could be due to the change in the lattice parameters after HP–HT. MFMMS scans were taken under FC conditions. For $PrSi_2$ the signal shows absorption minima at 11 K, same as the FM transitions (Figs. 2a). For the HP–HT samples, MFMMS response is flat in the temperature range (Fig. 2b), ruling out the presence of superconducting phases. No other features were observed in the temperature range studied. The minima-like behavior of these magnetic transitions can be explained in terms of the temperature dependence of the skin depth $\delta^2 = 2\sigma/\omega\mu$. The temperature dependence comes from the magnetic permeability $\mu(T)$ and the dc electrical conductivity $\sigma(T)$. Hence, an increase on the magnetic moment will show up as a minima-like behavior, as opposed to a superconductive transition which shows a sharp increase below the critical temperature [24].

3.2. Undoped Pr_5Si_3

HRXRD measurements of high Pr concentration samples were performed and a mixture of Pr_5Si_3 and Pr_3Si_2 phases was found.

a

b

a

b
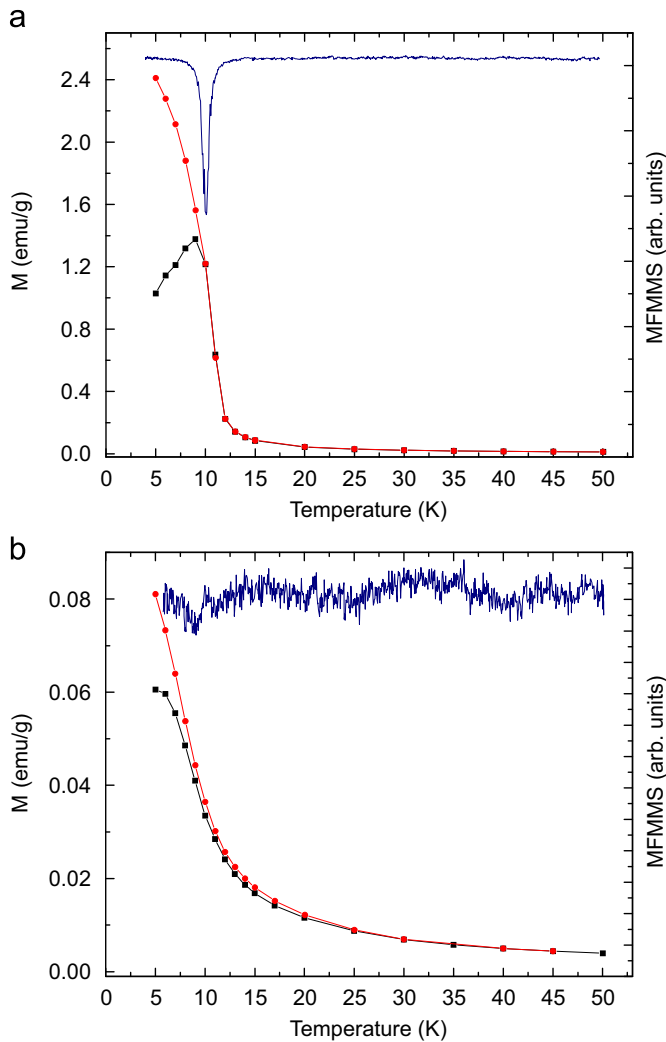
Fig. 2. ZFC (—■—) and FC (—●—) magnetization curves at 100 Oe; microwave absorption response as a function of temperature (solid blue line) for samples (a) $PrSi_2$ and (b) $PrSi_5$ (intended composition). (For interpretation of the references to color in this figure legend, the reader is referred to the web version of this article.)

Fig. 3. (a) Rietveld refinement profile of the HRXRD data for the undoped sample. Tick marks indicate reflections coming from the Pr_5Si_3 and Pr_3Si_2 phases. (b) Zoom of (a).

As was mentioned in the introduction, the existence of a Pr_3Si_2 phase was previously uncertain. We performed Rietveld refinement to obtain quantitative results from x-ray synchrotron data and confirmed the existence of the Pr_3Si_2 phase. Fig. 3a shows the observed and calculated diffraction profile for one of the undoped samples. The result of the refinement gives a "chi squared" value of $\chi^2 = 6.23$ and a "weighted profile R-factor" value of $R_{wp} = 0.159$.

Table 1 shows the structures, lattice parameters and phase weight fractions of the Pr_5Si_3 and Pr_3Si_2 phases after the refinement. Fig. 3(b) shows the HRXRD pattern focused around $Q = 2\ \text{Å}^{-1}$. In Fig. 3(a and b) the diffraction peaks coming from the Pr_5Si_3 and Pr_3Si_2 phases are indicated by tick marks. Only including the Pr_3Si_2 phase is possible to index all diffraction maxima and hence to obtain a good refinement. Thus, the presence of both phases (Pr_5Si_3 and Pr_3Si_2) and consequently the existence of Pr_3Si_2 are confirmed.

The magnetic characterization of the undoped sample (Fig. 4) shows that it is ferromagnetic at low temperatures and paramagnetic at high temperatures. The transition to a ferromagnetic order is at $T_C \sim 43$ K. This value agrees with that reported for Pr_5Si_3 single phase [5,6]. No other magnetic transitions have been observed, indicating that the Pr_3Si_2 phase does not show any ferromagnetic behavior. For Pr_5Si_3 single phase the saturation magnetization is

Table 1
Refined structures, lattice parameters and weight fraction of each different phase.

		Phase	
		Pr_5Si_3	Pr_3Si_2
Structure type		Tetragonal	Tetragonal
Space group		I 4/m C m (140)	P 4/m b m (127)
Unit cell parameters (Å)	a	7.814	7.765
	b	7.814	7.765
	c	13.754	4.36
Weight fraction (%)		87	13

$2.2\mu_B/$at [5]. For the samples studied here (Fig. 4a), at 10 K the saturation moment is 1.97 $\mu_B/$at. This value corresponds to a Pr_5Si_3 weight fraction of 89% in the samples, which is in good agreement with the Rietveld refinement results (Table 1).

3.3. Doped samples: $Pr_5Si_3B_x$ and $Pr_5Si_3C_x$

Fig. 5 shows the HRXRD patterns for the undoped sample and three samples doped with C and B. The addition of C gives rise to the appearance of several diffraction peaks not present in the undoped sample. This is an indication of the presence of multiple phases. The presence of multiple XRD maxima in the samples
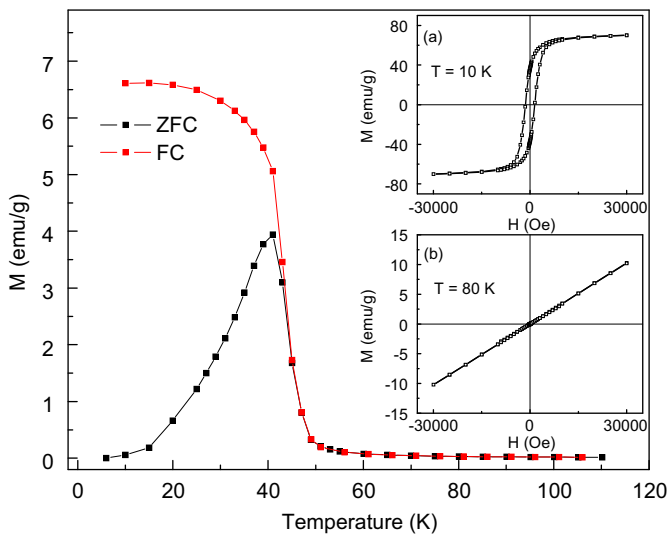
Fig. 4. ZFC (—■—) and FC (—●—) magnetization curves at 100 Oe for undoped sample. Insets: M vs. H at 10 K (a) and 80 K (b).
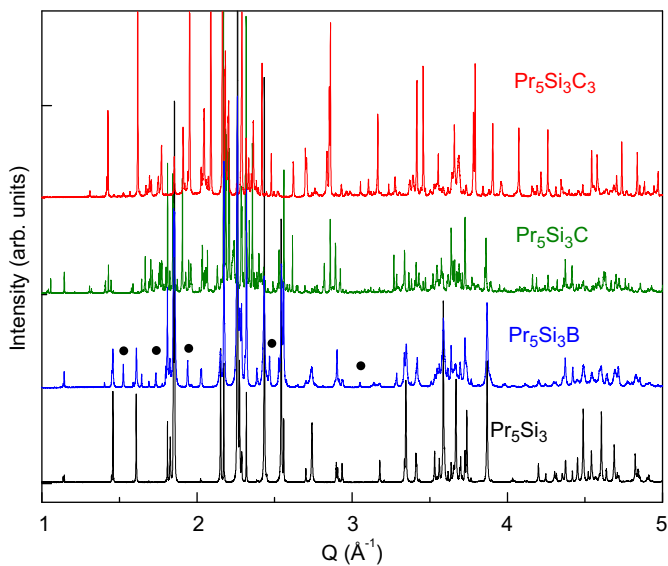
Fig. 5. HRXRD patterns for samples undoped Pr_5Si_3 (bottom black), Pr_5Si_3B (third to the top blue), Pr_5Si_3C (second to the top green) and $Pr_5Si_3C_3$ (top red). Dots indicate the PrB_4 diffraction maxima. (For interpretation of the references to color in this figure legend, the reader is referred to the web version of this article.)

makes identifying phases difficult. Therefore it is impossible to refine the structures. On the other hand, the addition of B produces new diffraction maxima that could be ascribed to the PrB_4 phase (marked as dots in Fig. 5).

The addition of B in the system does not alter the magnetic properties. However, the addition of C in the system gives rise to the presence of multiple ferromagnetic transitions. Fig. 6 shows the magnetization in ZFC–FC conditions and the MFMMS data for two representative Pr–Si–C samples. FM transitions occur at 52 and 80 K (Fig. 6a) and 20 and 66 K (Fig. 6b). MFMMS measurements show only minima at the same temperatures as the FM transitions, ruling out the existence of superconducting phases.

To identify the origin of the FM transitions we checked for the presence of other binary phases outside of the Pr-Si system: praseodymium oxides and praseodymium carbides as well as ternary compounds. Table 2 summarizes all the FM transitions found in the samples and shows the known binary (and ternary) Pr–Si–C phases which have FM transitions in those temperature
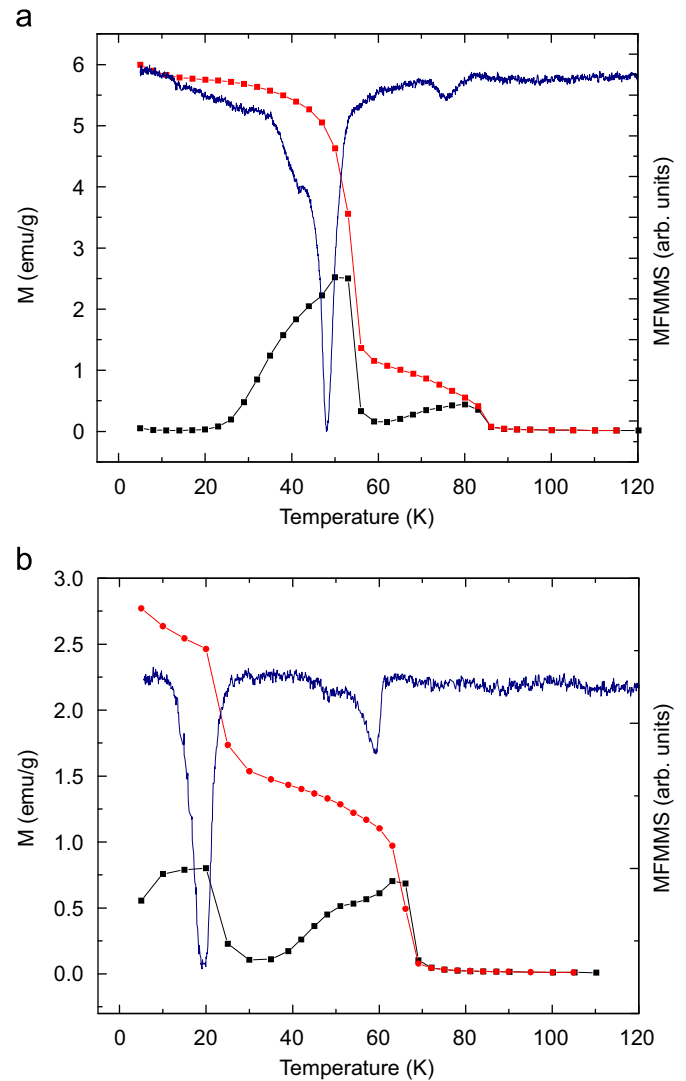
Fig. 6. ZFC (—■—) and FC (—●—) magnetization curves at 100 Oe; microwave absorption response as a function of temperature (solid blue line) for samples (a) $Pr_5Si_3C_{1.5}$ and (b) $Pr_5Si_3C_3$. (For interpretation of the references to color in this figure legend, the reader is referred to the web version of this article.)

ranges. According to the XRD patterns there are no indications that any of the binary oxides or carbides compounds are present in the samples. In addition none of these binary phases could explain the new magnetic transitions observed in the C doped samples. The oxides Pr_2O_3, Pr_7O_{12}, Pr_9O_{16}, Pr_5O_9, $Pr_{11}O_{20}$, Pr_6O_{11} show no cooperative magnetism, [25] while PrO_2 is antiferromagnetic with a Neel temperature of 14 K [26]. There are two antiferromagnetic carbides, Pr_2C_3 [27] with $T_N = 8$ K and PrC_2 [28] $T_N = 15$ K. For PrC_2 ferromagnetism has been also reported with $T_C = 7$ K [29].

$Pr_3Si_2C_2$ is the only ternary compound reported in literature. It is FM at low temperature, with a $T_C = 25$ K [30]. Fig. 7 shows the simulated diffraction pattern corresponding to this ternary phase and the experimental data for the sample with intended composition $Pr_5Si_3C_3$. In this sample the coexistence of $Pr_3Si_2C_2$ along with other phases is clear. Thus, the observed FM transition at 20 K is likely due to $Pr_3Si_2C_2$. This makes the magnetic transitions at 66 and 80 K the most interesting. These transitions might be related to the existence of new phases in the system because none of the Pr-silicides (or other ternary compounds) have transitions at these temperatures. Although Pr_3Si_4 has a FM transition at higher temperatures (~100 K), the presence of this Pr_3Si_4 phase is very unlikely according to XRD analysis.

Table 2
Observed FM transitions divided in three temperature ranges. The corresponding Pr-Si binary (or ternary) phases having transition at the same temperatures are indicated.

Compound (intended composition)	First magnetic transition ($T < 40$ K)	Possible phase from literature	Second magnetic transition (40 K $< T < 60$ K)	Possible phase from literature	Third magnetic transition ($T > 60$ K)	Possible phase from literature
Pr_5Si_3	No	–	43 K	Pr_5Si_3	No	–
$Pr_5Si_3B_{0.3}$	No	–	43 K	Pr_5Si_3	No	–
Pr_5Si_3B	No	–	43 K	Pr_5Si_3	No	–
$Pr_5Si_3C_{0.3}$	20 K	$Pr_3Si_2C_2$	43 K	Pr_5Si_3	80 K	Unknown
Pr_5Si_3C	20 K	$Pr_3Si_2C_2$	52 K	PrSi	80 K	Unknown
$Pr_5Si_3C_{1.5}$	No	–	52 K	PrSi	80 K	Unknown
$Pr_5Si_3C_2$	20 K	$Pr_3Si_2C_2$	43 K	Pr_5Si_3	66 K	Unknown
$Pr_5Si_3C_3$	20 K	$Pr_3Si_2C_2$	No	–	66 K	Unknown
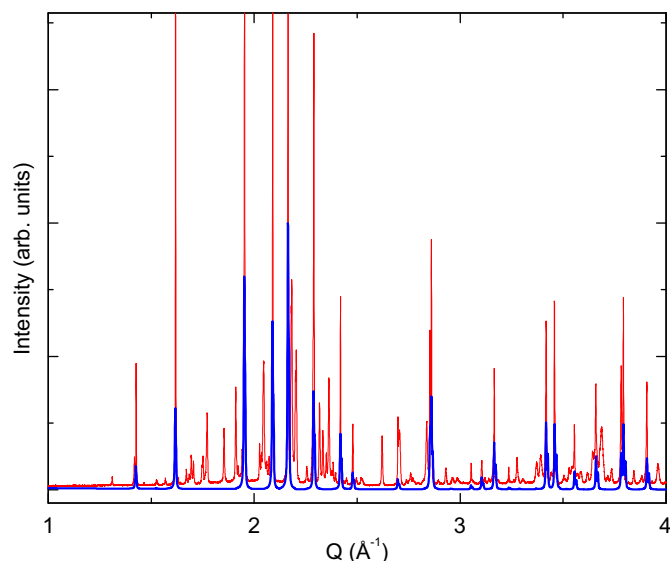
Fig. 7. X-ray diffraction patterns for sample $Pr_5Si_3C_3$ (thin red lines). Simulated X-ray diffraction pattern for phase $Pr_3Si_2C_2$ (thick blue lines). (For interpretation of the references to color in this figure legend, the reader is referred to the web version of this article.)

4. Conclusions

We have investigated structural and magnetic properties in the Pr–Si system in two different regions of the phase diagram. The highest Pr concentration area was doped with C and B. In the $PrSi_2$ compounds we used HP–HT synthesis. Fast screening using MFMMS measurements indicates the absence of superconductivity in our samples. The addition of C to the Pr_5Si_3 phase gives rises to several phases and new magnetic transitions. Unfortunately, the XRD patterns for C doped samples show multiple peaks and the identification of new phases was not possible. Doping the system with B creates a PrB_4 phase and no new magnetic transitions have been observed. XRD studies and Rietveld refinement of undoped sample confirm the existence of the so far elusive Pr_3Si_2 phase.

Acknowledgments

References

[1] J. de la Venta, Ali C. Basaran, T. Grant, A.J.S. Machado, M.R. Suchomel, R.T. Weber, Z. Fisk, Ivan K. Schuller, Superconductor Science and Technology 24 (2011) 075017.
[2] T.B. Massalski, Binary Alloy Phase Diagrams, Materials Information Society, Materials Park, Ohio, 1990.
[3] E.I. Gladyshevskii, Izvestiya Akademii Nauk SSSR: Neorganic Materials 5 (1965) 706.
[4] N.P. Gorbachuk, A.S. Bolgar, A.V. Blinder, Powder Metallurgy and Metal Ceramics 36 (1997) 498.
[5] N. Pinguet, F. Weitzer, K. Hiebl, J.C. Schuster, H. Noël, Journal of Alloys and Compounds 348 (2003) 1.
[6] D. Souptel, A. Leithe-Jasper, W. Löser, W. Schnelle, H. Borrmann, G. Behr, Journal of Crystal Growth 273 (2004) 311.
[7] A. Iandelli, A. Palenzona, Handbook of Physics and Chemistry of Rare Earths, Vol. 2, Elsevier, Amsterdam, 1979.
[8] V.N. Nguyen, F. Tcheou, J. Rossat-Mignod, Solid State Communications 23 (1977) 821.
[9] P. Schobinger-Papamantellos, K.H.J. Buschow, P. Fischer, Journal of Magnetism and Magnetic Materials 114 (1992) 131.
[10] V.N. Eremenko, K.A. Meleshevich, Y.I. Buyanov, I.M. Obushenko, Doklady Akademii Nauk Ukrainskoj SSR (A) 11 (1984) 80.
[11] A.B. Gokhale, A. Munitz, G.J. Abbaschian, Bulletin of Alloy Phase Diagrams 10 (1989) 246.
[12] I.I. Mazin, Nature 464 (2010) 183.
[13] M.A. Alario-Franco, High-temperature superconductivity, McGraw-Hill Encyclopedia of Science and TechnologyMcGraw-Hill, New York, 2007.
[14] S. Yamanaka, S. Izumi, S. Maekawa, K. Umemoto K, Journal of Solid State Chemistry 182 (2009) 1991.
[15] J. Wang, B.H. Toby, P.L. Lee, L. Ribaud, S. Antao, C. Kurtz, M. Ramanathan, R.B. Von Dreele, M.A. Beno, Review of Scientific Instruments 79 (2008) 085105.
[16] P.L. Lee, D. Shu, M. Ramanathan, C. Preissner, J. Wang, M.A. Beno, R.B. Von Dreele, L. Ribaud, C. Kurtz, S.M. Antao, X. Jiao, B.H. Toby, Journal of Synchrotron Radiation 15 (2008) 427.
[17] L.R. Dalesio, J.O. Hill, M. Kraimer, S. Lewis, D. Murray, S. Hunt, W. Watson, M. Clausen, J. Dalesio, Nuclear Instruments and Methods A 352 (1994) 179.
[18] B.H. Toby, Journal of Applied Crystallography 34 (2001) 210.
[19] A.C. Larson, R.B. Von Dreele, General Structure Analysis System (GSAS), Los Alamos National Laboratory Report LAUR 86, 748 (2000).
[20] J.G. Ramirez, Ali C. Basaran, J. de la Venta, Juan Pereiro, Ivan K. Schuller (unpublished).
[21] B.F. Kim, J. Bohandy, K. Moorjani, F.J. Adrian, Journal of Applied Physics 63 (1988) 2029.
[22] J. Hopkinson, Proceedings of the Royal Society of London 48 (1890) 1.
[23] S. Chikazumi, Physics of Ferromagnetism, Oxford University Press, Oxford, 1997 486.
[24] D.N. Peligrad, B. Nebendahl, C. Kessler, M. Mehring, A. Dulčić, M. Požek, D. Paar, Physical Review B 58 (1998) 11652.
[25] S. Kern, Journal of Chemical Physics 40 (1964) 208.
[26] J.B. MacChesney, H.J. Williams, R.C. Sherwood, F. Potter, Journal of Chemical Physics 41 (1964) 3177.
[27] M. Atoji, J. Solid State Chem. 26 (1978) 51.
[28] M. Atoji, Journal of Chemical Physics 46 (1967) 1891.
[29] T. Sakai, G. Adachi, T. Yoshida, J. Shiokawa, Journal of Chemical Physics 75 (1981) 3027.
[30] M.H. Gerdes, A.M. Witte, W. Jeitschko, A. Lang, Bernd Künnen, Journal of Solid State Chemistry 138 (1998) 201.